

# Numerical Simulation of Flow Field in Coaxial Tank Gun Recoil Damper

W. Elsaady<sup>1</sup>, A. Ibrahim<sup>2\*</sup> and A. Abdalla<sup>3</sup>

<sup>1</sup> The University of Manchester, M13 9PL, Manchester, UK

<sup>2</sup> Military Technical College, 11766 Cairo, Egypt

<sup>3</sup> Modern Academy for Science and Technology, 11742 Cairo, Egypt

The manuscript was received on 22 January 2019 and was accepted  
after revision for publication on 18 May 2019.

## Abstract:

*To know the hydraulic resistance of tank gun hydraulic damper is essential to determine the barrel recoil parameters. Usage of one-dimensional analytical models simplifies the determination of the hydraulic resistance; however these models do not provide data about the flow nature inside the hydraulic damper. This paper studies the internal flow inside the hydraulic damper of the gun recoil system. The dynamic mesh technique using two-dimensional flow computational solver has been used. A User Defined Function (UDF) has been developed to feed the solver by the measured recoil velocity. The study shows that the liquid flow inside the hydraulic damper is complicated at the start of the gun recoil and it is quickly changing to a simpler flow pattern until the end of the recoil. Also, the liquid pressure inside the hydraulic damper has been measured and compared to the computational values.*

## Keywords:

*coaxial recoil system, dynamic mesh, hydraulic damper, recoil simulation*

## 1. Introduction

A coaxial hydraulic damper is embedded around the barrel of a tank gun to attenuate the kinetic energy transferred to the recoiling parts due to firing. It simultaneously provides the necessary energy to return the recoiling parts into their initial position. The coaxial hydraulic damper consists of two main parts, namely the hydraulic brake and the recuperator. The hydraulic brake provides the necessary hydraulic resistance, which arises from forcing the hydraulic liquid to be throttled through very narrow areas during recoil cycle. The recoil cycle reduces the resultant force on the tank turret. This force disadvantageously affects the tank stability during firing. Some of the

---

\* Corresponding author: Department of Weapons and Ammunition, Military Technical College, 11766 Cairo, Egypt. Phone: +20 106 255 9882, E-mail: a.ibrahim@mtc.edu.eg

recoil energy is stored in the recuperator, which is merely a helical spring, to return the recoiling parts into their initial position.

The coaxial hydraulic damper under investigation consists of a spring recuperator and simple recoil brake as shown in Fig. 1. The recuperator spring is placed around the recoil brake piston. The recoil brake cylinder is filled with working liquid. Also, it works as cylindrical guide for the barrel assembly. A front cushioning is employed for smoothing the impact on the front part of hydraulic damper at the end of counter-recoil.

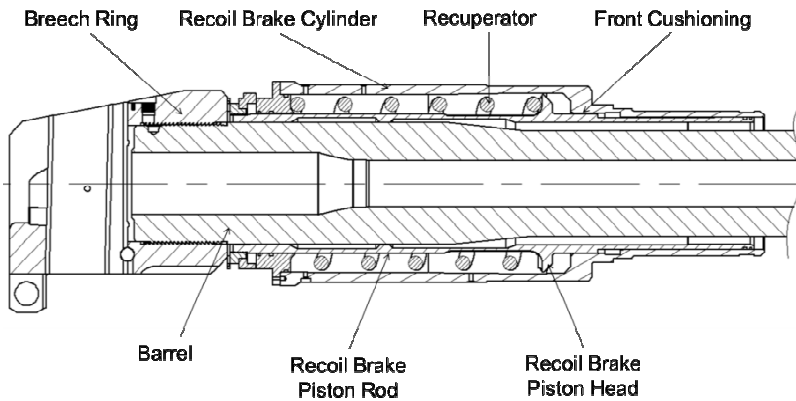


Fig. 1 Construction of coaxial hydraulic damper

Fig. 2 illustrates the function during recoil where the piston recoils with barrel allowing the hydraulic liquid to be throttled through the annular area around the piston head causing an increase of the liquid pressure in space (1). The pressure difference between the liquid in spaces (1) and (2) provides the necessary hydraulic resistance during recoil.

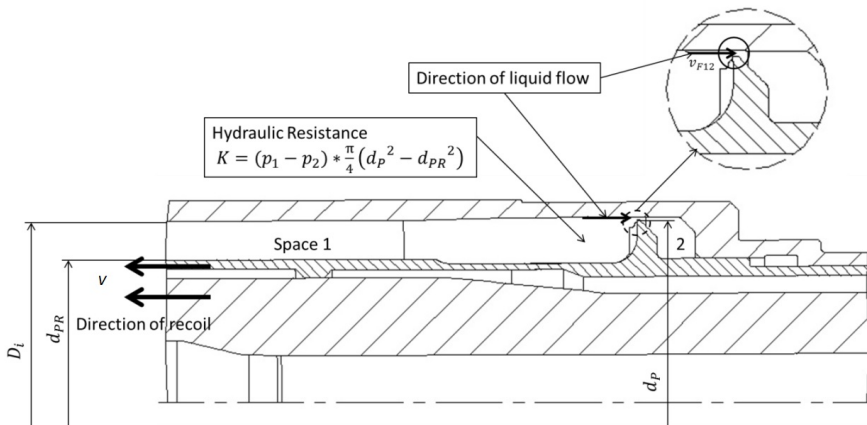


Fig. 2 Function of coaxial hydraulic damper during recoil

Aboul et al. [1] studied the recoil cycle of the 57mm anti-tank gun using one-dimensional model. The study investigated the effect of wear in the inner diameter

of the recoil brake throttling ring and counter recoil piston on the dynamic behaviour of the recoil cycle. Hussein [2] also used a one-dimensional model to investigate the effect of some constructional parameters on the dynamics of the gun recoil system. The study was applied to the recoil cycle of the 115mm main gun of T-62 battle tank.

Xiaodong et al. [3, 4] studied the recoil system of the 155mm caliber self-propelled howitzer model M109 to obtain its recoil parameters. The one-dimension equation of motion of recoiling parts during recoil is written as:

$$m_R \frac{d^2 x}{dt^2} = m_R \frac{dv}{dt} = P_B - K - P_R - R_f + m_R g \sin \phi, \quad (1)$$

where  $m_R$  is the mass of recoiling parts;  $x$  is the recoil distance;  $v$  is the recoil velocity;  $P_B$  is the driving force due to firing;  $K$  is the hydraulic resistance during recoil;  $P_R$  is the recuperator spring force,  $R_f$  is the friction resistances in the barrel guides and the hydraulic damper stuffing boxes, and  $\phi$  is the angle of elevation of the gun barrel. Also, they used two different optimization techniques to modify some hydraulic coefficients to change the theoretical recoil distance according to the measured values.

Songjiang et al. [5] studied the dynamic changes of the internal flow field inside the hydraulic damper using 3D dynamic meshing technique in Ansys/Fluent. When comparing their results with the experimental work, a significant difference has been reported. This difference could be due to the increase of working domain volume during simulation where a cavity (under-pressure zone) is supposed to be formulated in front of the piston head. This cavity, which physically has the form of compressible liquid-vapor mixture, has been replaced by an incompressible liquid in their Computational Fluid Dynamics (CFD) model for simplification.

Xiaodong et al. [6] simulated the gun recoil cycle using Ansys/Fluent in collaborative MATLAB model. The comparison between the computational and experimental results proved that their method is feasible and valid.

In majority, the available literature that studies gun recoil is based on analytical one-dimensional models. However, numerical investigations conducted via CFD techniques are rarely found. Herein, the flow field in the tank gun recoil damper, shown in Fig. 1, is discussed applying Reynolds Averaged Navier-Stokes (RANS) equations in time-dependent form exploiting the computational facilities of Ansys/Fluent.

## 2. Experimental Work

The experimental work has been carried out in Egyptian Central Shooting Ranges (ECSR) of the ministry of military production. The experiments are aiming to measure the pressure inside the coaxial hydraulic damper and the velocity of the recoiling parts with time. The measuring system is schematically shown in Fig. 3. It consists of:

- a piezo-electric pressure transducer screwed to recoil brake cylinder body at the location of replenishing hose fixation screw,
- two piezo-electric pressure transducers are screwed to two different locations of the barrel. The rear transducer is placed at 8.9 cm from the rear face of the barrel to record the breech pressure, while the front is placed at 47 cm to record the shoulder pressure,
- a charge amplifier and data acquisition system (DAQ) connected to LabVIEW measuring software,
- a high speed camera to record the recoil cycle using Phantom software.

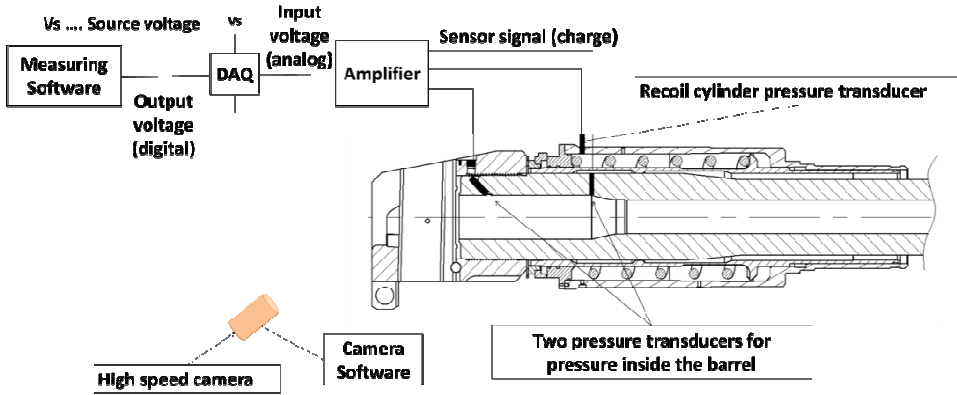


Fig. 3 Illustration of the measuring system

The gun assembly is shown in Fig. 4. The data that are recorded using the high speed camera are processed to obtain the recoil velocity with time. The measured values of the recoil velocity are fed to the CFD solver through the UDF. The shoulder pressure, which is measured by the front transducer, fitted inside the barrel, is very important to check the formation of pressure wave, which may be generated by a partial ignition of propellant at the breech side [7, 8].



Fig. 4 Gun assembly

### 3. Computational Work

#### 3.1. Governing Equations

The computational investigation is carried out by applying RANS equations in time-dependent form. The first-order upwind scheme is used in discretizing the spatial dependent properties since the dynamic mesh technique utilizes the first order schemes in Ansys/Fluent. In RANS equations, the solution is decomposed into the mean and fluctuating components. The mean-flow equations are the averaged momentum equation [9],

$$\frac{\partial u_i}{\partial t} + u_j \frac{\partial u_j}{\partial x_j} = -\frac{1}{\rho} \frac{\partial p}{\partial x_i} + \nu_L \frac{\partial^2 u_i}{\partial x_j^2} - \frac{\partial u_i u_j}{\partial x_j}. \quad (2)$$

The computations adopt the SIMPLE algorithm coupled with Re-Normalization Group (RNG  $k-\varepsilon$ ) two-equation turbulence model with enhanced wall function [10]. This model has been developed to deal with rapidly strained swirling flows. The turbulent energy and dissipation rate equations of RNG  $k-\varepsilon$  model can be written as the following:

$$\frac{\partial(\rho k)}{\partial t} + \frac{\partial(\rho k u_i)}{\partial x_i} = \frac{\partial}{\partial x_j} \left[ \alpha_k \mu_{\text{eff}} \frac{\partial k}{\partial x_j} \right] + \mu_t S^2 - \rho \varepsilon, \tag{3}$$

$$\frac{\partial(\rho \varepsilon)}{\partial t} + \frac{\partial(\rho \varepsilon u_i)}{\partial x_i} = \frac{\partial}{\partial x_j} \left[ \alpha_\varepsilon \mu_{\text{eff}} \frac{\partial \varepsilon}{\partial x_j} \right] + C_{1\varepsilon} \frac{\varepsilon}{k} \mu_t S^2 - C_{2\varepsilon} \rho \frac{\varepsilon^2}{k}, \tag{4}$$

where  $\rho$  is the liquid density,  $k$  is the turbulent energy,  $\varepsilon$  is the dissipation rate,  $u_i$  is the velocity component,  $\mu_{\text{eff}}$  is the effective viscosity,  $\mu_t$  is the turbulent viscosity,  $S$  is the modulus of the mean rate of strain tensor and  $C_{1\varepsilon}$  and  $C_{2\varepsilon}$  are two constants of the turbulence model. The parameters  $\alpha_k$  and  $\alpha_\varepsilon$  are the inverse effective Prandtl numbers for  $k$  and  $\varepsilon$ , respectively.

### 3.2. Dynamic Layering

The layering method in Ansys/Fluent is based on adding or eliminating cells on the boundaries during their movement. It adopts only the cells of quad shape in case of 2D problems or wedge/hexahedral shapes in case of 3D problems. Dynamic layering can be of height-based or ratio-based type. Cells are added when the fluid zone grows or they are deleted as it shrinks. In height-based layering, it is required to set an ideal height ( $h_{\text{ideal}}$ ) of grids as shown in Fig. 5. The value of ideal height should be chosen close to the height of the wall adjacent cell ( $h_{\text{adj}}$ ), therefore the moving boundary cannot go through more than one cell in each time step.

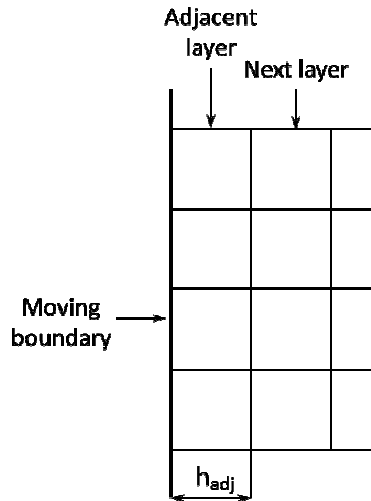


Fig. 5 Dynamic layering grid

When the fluid zone grows, the cell is split according to Eq. (5); and when the fluid zone shrinks, the cell is deleted according to Eq. (6).

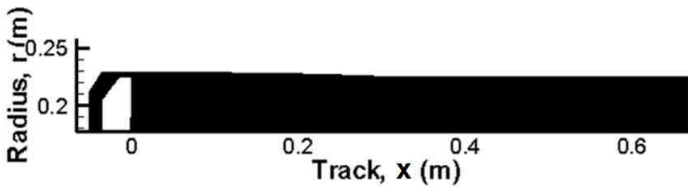
$$h_{\text{adj}} > (1 + \alpha_s) h_{\text{ideal}}, \quad (5)$$

$$h_{\text{adj}} > \alpha_c h_{\text{ideal}}, \quad (6)$$

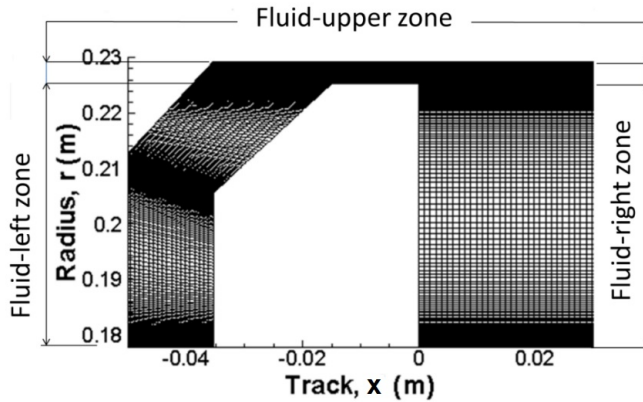
where  $\alpha_s$  and  $\alpha_c$  are the split and collapse factors, respectively.

### 3.3. Grid Generation

Since the computational domain of hydraulic damper is axisymmetric, one half of it is chosen as shown in Fig. 6a. It is comprised of three main zones; fluid-right, fluid-left and fluid-upper, as shown in Fig. 6b. The fluid-right and fluid-left zones represent the flow field behind and in front of the piston head, respectively. The fluid-upper zone is a narrow zone representing the throttling area around the recoil brake piston head. This zone is separated from other zones by interface boundaries.



a) Computational domain



b) Generated grid around the piston head

Fig. 6 Construction of the computational domain

The grid sensitivity study has been carried out using four grids to obtain the grid independent solution. The coarsest grid consists of 150 000 cells, while the finest one consists of 888 000 cells. The number of cells is increased from the coarsest grid to the finest one such that the dimensionless wall distance  $y^+$  is less than 1.0. Since the fluid pressure in space (1) is of main concern in this study, it is taken as a decisive parameter of the grid choice. The variation of this pressure versus time for the generated grids is shown in Fig. 7. The used grid in this model is the third one since there is insignificant change of the pressure by increasing the grid size.

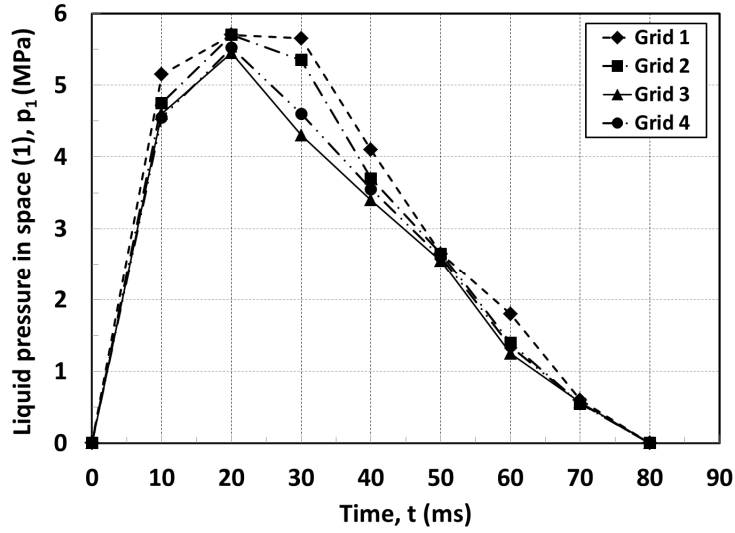


Fig. 7 Variation of the pressure in space (1) with time using four grids

**3.4. Boundary Conditions**

The simulation is initialized at zero operating pressure neglecting the gravity effect. For the recoiled boundaries, the data of measured recoil velocity are fit to a set of polynomial equations, which are compiled to the CFD solver using UDF. Fig. 8 depicts the change of measured recoil velocity and the fitted data with time. From this figure, it can be noticed that fitted and measured data are almost the same.

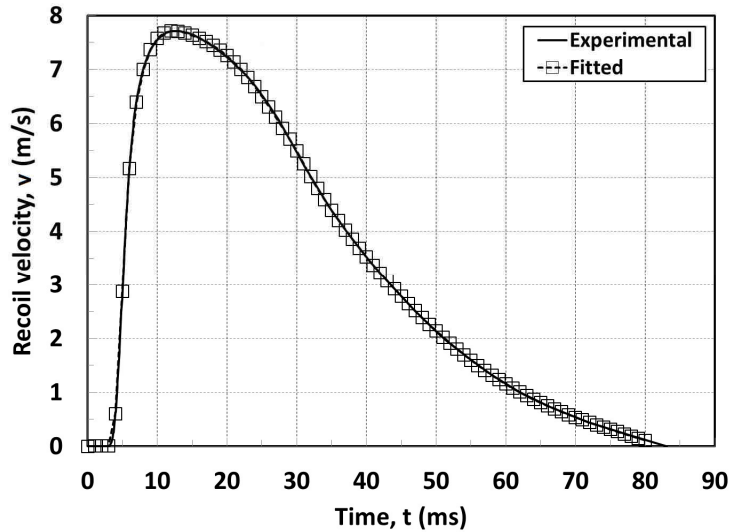


Fig. 8 Experimental and fitted data of recoil velocity versus time

The dynamic mesh zones and mesh interfaces are shown in Fig. 9. All boundaries are defined as adiabatic walls except the boundaries between the fluid zones and the upper wall of piston head denoted by (r9) is defined as interfaces. The wall boundaries (r7 and r10) are defined as rigid bodies in the dynamic mesh zones.

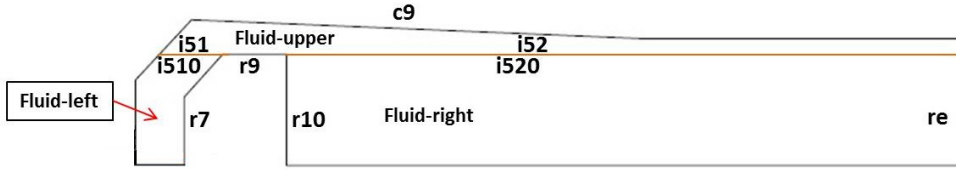


Fig. 9 Dynamic mesh zones and their boundaries

#### 4. Results and Discussions

Fig. 10 illustrates the experimental and computational values of liquid pressure in space (1) with time. It can be noticed that the trend of measured and computational values are approximately the same. However, there are discrepancies between the measured values and the computational ones, which could be reasoned out due to the following assumptions: (1) replacement of the recuperator spring with liquid in the computational domain, (2) neglecting the formation of vacuum in front of the piston head, during recoil, and replacing it with working liquid and (3) ignoring the gas-fluid mixture compressibility.

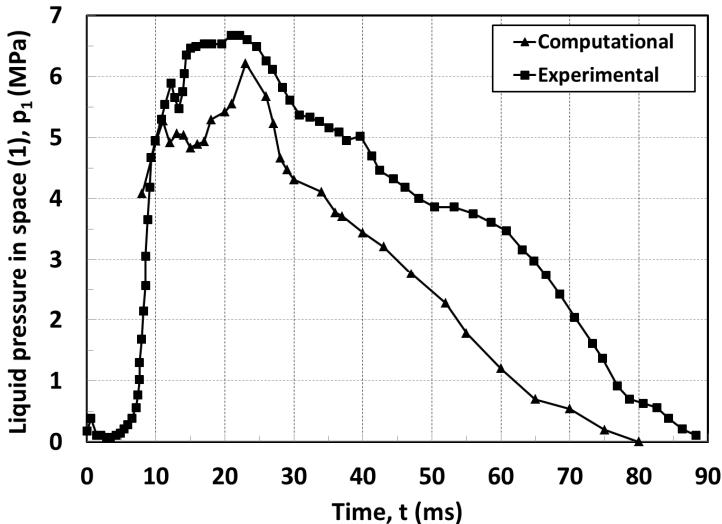
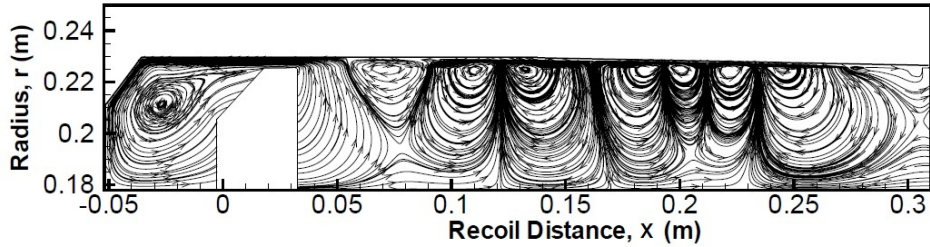


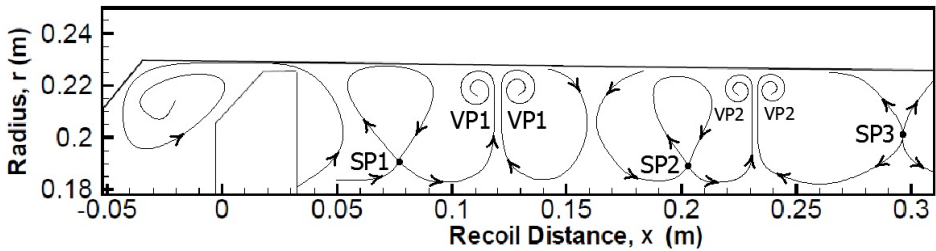
Fig. 10 Computational and experimental data of liquid pressure in space (1)

Fig. 11 displays the streamlines of the liquid flow inside the recoil brake at time  $t = 0.01$  s. Due to the flow interaction between the liquid, which leaves from the right side of the piston head to the left side and the remaining liquid, a vortex structure is generated resulting in a saddle point SPI. Consequently, a vortex pair VPI is formed;

then a vortex structure forming a saddle point SP2 followed by a vortex pair VP2 and so on. At the same time, a large primary vortex rotating in a counter clockwise direction is formed in front of the piston head. The core of this vortex is located at a distance of 22 mm in front of the piston head.



a) Stream traces



b) Sketch of stream traces

Fig. 11 Velocity stream traces and its structure at  $t = 0.01$  s

Fig. 12 depicts the stream traces of the liquid flow inside the recoil brake at time  $t = 0.02$  s. Due to the high acceleration of the piston at this moment, it can be noticed that there are a lot of disturbances behind the piston head resulting in disappearing of the saddle point SP1. Also, these disturbances contribute in changing the locations of cores of vortices VP1 and VP2 as well as the location of saddle point SP2. In front of the piston head, the position of the primary vortex core moves towards the piston head and a secondary vortex generates in clockwise direction.

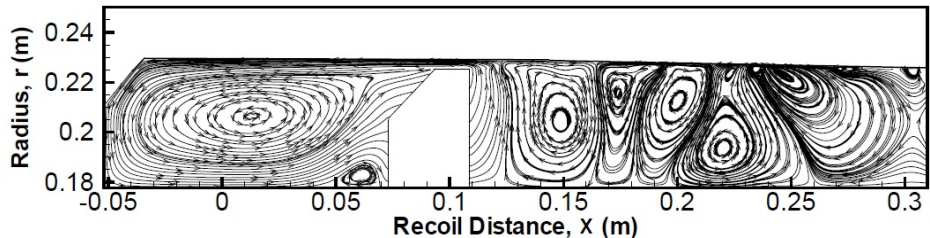
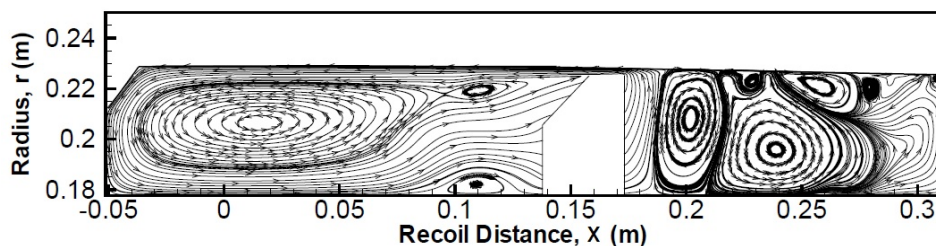


Fig. 12 Velocity stream traces at  $t = 0.02$  s

Fig. 13 illustrates the streamlines of the liquid flow inside the recoil brake at time  $t = 0.03$  s. At this moment, the piston moves under a decelerating force. Therefore, the vortices behind the piston head are of lower number and bigger structure. A saddle

point is generated between the primary vortex in front of the piston head and the small vortex beside the upper wall. However, there is an insignificant shift of the position of the primary vortex core and the secondary vortex still exists.



*Fig. 13 Velocity stream traces at  $t = 0.03$  s*

Fig. 14 displays the development of the flow inside the recoil brake from the moment at  $t = 0.04$  s to the end of the recoil at  $t = 0.08$  s. It can be noticed that there is an insignificant change of the position of the primary vortex core in front of the piston head. This insignificant change is due to the decelerating motion of the recoiling parts, which helps in decreasing the flow rate of the liquid towards the front side of the piston head. In front of the piston head, both the saddle point and the secondary vortex vanished. However, due to the inertia of the liquid in front of the piston head, a new secondary vortex starts formation at  $t = 0.05$  s. At the moment of recoil end, this secondary vortex is completely formed.

## 5. Conclusions

Although one-dimensional analytical models are very simple compared to CFD solutions, they do not give any idea about the flow field inside the hydraulic damper. The current computational study clarifies the history of liquid flow field inside the hydraulic damper during recoil. Moreover, despite the ignorance of fluid compressibility due to the presence of liquid vapor as two-phase flow, the presented model determines the hydraulic pressure time history with acceptable accuracy in terms of the maximum value. This could be sufficient for manufacturing requirements. The impact of changing the geometry of the piston head and the throttling area on the liquid flow could be investigated following the procedures of the current study. This helps in getting lower turbulence of the flow resulting in smooth motion of the recoiling parts, especially at the start of recoil.

## Acknowledgement

The authors would like to thanks the staff of ECSR for the valuable technical support during conducting the experimental work.

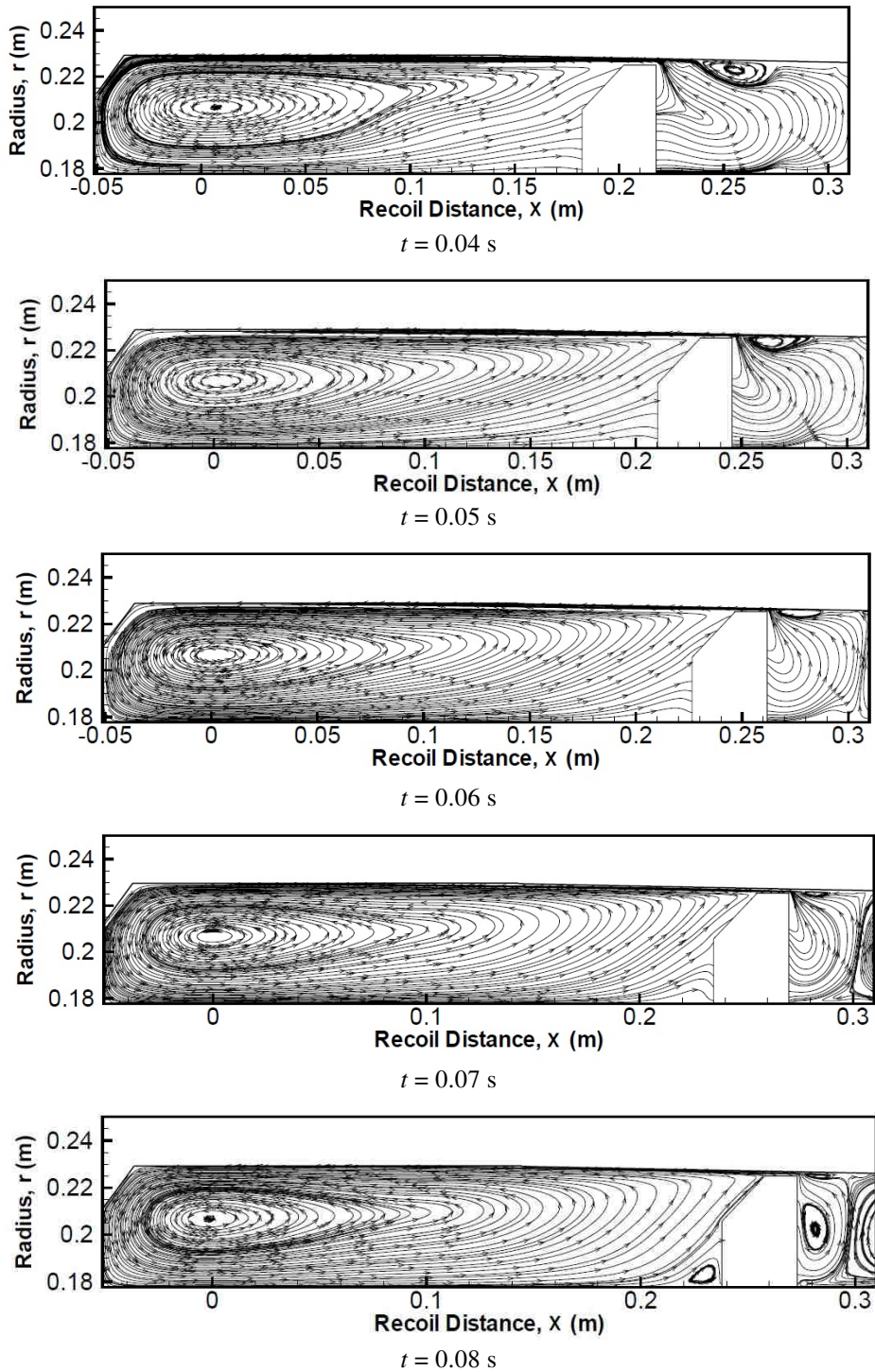


Fig. 14 Velocity stream traces at time duration starting from  $t = 0.04$  s to  $t = 0.08$  s

## References

- [1] ABOUL, M.H., SALEH, I. and TAHA, S. The Regressive Method of Solution of Gun Recoil Cycle. In *Proceedings of 2<sup>nd</sup> International Conference on Applied Mechanics and Mechanical Engineering (AMME)*. Cairo: Military Technical College Press, 1986, p. 89-99.
- [2] HUSSEIN, A. *Investigation of the Effect of Constructional Parameters on the Dynamics of Gun Recoil System* (in Egyptian) [MSc. Thesis]. Cairo: Military Technical College, 2002.
- [3] XIAO-DONG, Z., JIAN-PING, F., CHENG, W. and GUOJIE, K.A. Method of Recoil Brake Interior Chamber Pressure Test and Calculation on Gun's Recoiling Impact. In *Proceedings of 9<sup>th</sup> International Conference on Electronic Measurement and Instruments (ICEMI)*, Beijing: IEEE, 2009, p. 713-717. DOI 10.1109/ICEMI.2009.5274450.
- [4] XIAO-DONG, Z., PEI-LIN, Z., JIAN-PING, F. and CHENG, W. Research on According Calculation of Hydraulic Resistance Coefficients of Recoil Brakes of Gun Based on Improved Genetic Algorithm. In *Proceedings of International Conference on Measuring Technology and Mechatronics Automation (ICMTMA)*, Zhangjiajie, Hunan: IEEE, 2009, p. 281-284. DOI 10.1109/ICMTMA.2009.552.
- [5] SONGJIANG, P., CHENG, Z. and CUNGUI, Y. The Numerical Simulation of Three-Dimensional Dynamic-Mesh Flow Field of a Hydraulic Buffer. *Advanced Materials Research*, 2012, vol. 588-589, p. 1264-1268. DOI 10.4028/www.scientific.net/AMR.588-589.1264.
- [6] XIAO-DONG, Z., PEI-LIN, Z., JIAN-PING, F. and CHENG, W. Collaborative Simulation Technology Based on Matlab/Fluent. *Computer Engineering*, 2010, vol. 35, no. 20, p. 220-224. ISSN 1000-3428.
- [7] NAKAMURA, Y., ISHIDA, T., MIURA, H. and MATSUO, A. Negative Differential Pressure by Ignition of Granular Solid Propellant. In *Proceedings of International Symposium on Ballistics*. Tarragona, 2007, p. 473-480. [cited 2018-12-06]. Available from: [http://ciar.org/~ttk/mbt/papers/isb2007/paper.x.isb2007.IB29.negative\\_differential\\_pressure\\_by\\_ignition\\_of\\_granular\\_solid\\_propellant.nakamura\\_ishida\\_miura\\_matsuo.2007.pdf](http://ciar.org/~ttk/mbt/papers/isb2007/paper.x.isb2007.IB29.negative_differential_pressure_by_ignition_of_granular_solid_propellant.nakamura_ishida_miura_matsuo.2007.pdf).
- [8] JANG, J., SUNG, H., ROH, T. and CHOI, D. Numerical Study on Properties of Interior Ballistics According to Solid Propellant Position in Chamber. In *Proceedings of 26<sup>th</sup> International Symposium on Ballistics*. Miami: A DESTech Publications, 2011, p. 721-730. ISBN 978-1-60595-052-5.
- [9] KUNDU, P. *Fluid Mechanics*. 2<sup>nd</sup> ed. San Diego: Academic Press, 1990, 638 p. ISBN 0-12-428770-0.
- [10] ORSZAG, S., YAKHOT, V., FLANNERY, W. and BOYSAN, F. Renormalization Group Modeling and Turbulence Simulations. In *International Conference on Near-Wall Turbulent Flows*. Tempe, Arizona: Elsevier, 1993, p. 1031. ISBN 0-444-89663-5.